JOURNAL OF SOLID STATE CHEMISTRY **131,** 399–404 (1996)
ARTICLE NO. SC977421

Synthesis and Structure of a New Quaternary Rare-Earth Sulfide, $La_6MgGe_2S_{14}$, and the Related Compound $La_6MgSi_2S_{14}$

Robert L. Gitzendanner, Courtney M. Spencer, and Francis J. DiSalvo*

Department of Chemistry, Cornell University, Ithaca, New York 14853-1301

and

Michael A. Pell and James A. Ibers

Department of Chemistry, Northwestern University, Evanston, Illinois 60208-3113

Received March 3, 1997; in revised form April 9, 1997; accepted April 10, 1997

A new quaternary rare-earth sulfide has been isolated and identified. Crystals of $La_6MgGe_2S_{14}$, as well as of the previously identified $La_6MgSi_2S_{14}$ have been grown from a mixed binary-halide eutectic flux. They both crystallize in the hexagonal space group C_6^6-$P6_3$, with $Z = 1$. The crystal structures of these compounds have been determined by single-crystal X-ray diffraction techniques. Crystal data are $La_6MgGe_2S_{14}$ – $a = 10.367(1)$ Å, $c = 5.814(1)$ Å ($T = 298$ K), $V = 541.09(8)$ Å^3, $R_w(F^2) = 0.050$, R_1 (on F) $= 0.018$; $La_6MgSi_2S_{14}$ – $a = 10.363(2)$ Å, $c = 5.742(1)$ Å ($T = 298$ K), $V = 534.1(2)$ Å^3, $R_w(F^2) = 0.058$, and R_1 (on F) $= 0.022$. Structurally, these compounds belong to the $Ln_6M_2M'_2S_{14}$ family (Ln = rare-earth, M = first-row transition metal or main-group metal, M' = main-group metal). Their structures are characterized by one-dimensional chains of MS_6 face-sharing octahedra running parallel to the 6_3 axis, surrounded by isolated $M'S_4$ tetrahedra aligned along the three-fold axes. © 1997 Academic Press

INTRODUCTION

Nonlinear optical (NLO) materials are being developed for many applications including optical storage and switching as well as frequency doubling (1). Ideal NLO materials must satisfy a long list of requirements, and for each application this "wish list" is different. Ideal properties include a significant NLO susceptibility; transparency in the regime(s) of interest (both ω and 2ω for frequency doubling applications); high resistance to optical damage; and mechanical, chemical, and thermal stability, as well as ease of doping and processing. Currently, no known material is optimal in all categories for all uses. Thus, the search for new and perhaps better NLO materials continues.

* To whom correspondence should be addressed.

Sulfides are not commonly studied for such applications as they tend to form materials with smaller band gaps than oxides, and thus are more likely to be absorbing at shorter wavelengths. However, when compared to oxide materials, sulfides typically have a wider transmission window in the infrared region (out to $\lambda \cong 14$ μm for $CaLa_2S_4$ (2)), making them useful in certain applications. Certain binary sulfide phases, such as ZnS and La_2S_3 (3), have already been shown to be potentially useful as infrared optical materials. Some nonlinear optical ternary sulfide materials, such as $AgGaS_2$, are known (4, 5). Several quaternary rare-earth sulfides and even a quinary compound with structural and optical properties that warrant further investigation as NLO materials have been identified (6, 7).

In our investigations we attempted to tune the structure, stability, and polarizability of our materials by carefully selecting the component elements. We started with the early lanthanides because of the apparent ability of rare-earth metals to impart thermal stability to sulfides (8). The highly electropositive alkali metals and alkaline-earth metals provide for greater ionic interactions and higher polarizablity. In sulfides, the rare-earth metals are commonly found in either cubic or octahedral coordination geometries and the alkali metals and alkaline-earth metals normally adopt an octahedral coordination (9, 10). Since these coordination environments are intrinsically centrosymmetric, main-group elements (M' = Si and Ge), which prefer noncentrosymmetric tetrahedral coordination in sulfides, were incorporated in an attempt to break the inversion symmetry. Because single crystals of sulfides have been grown from a variety of molten fluxes (6, 9, 11–13), we used eutectic fluxes of mixed alkali metal/alkaline-earth binary halides in the present studies.

The $Ln_6M_2M'_2S_{14}$ family of compounds is extensive (14–22). The basic structure is of $Al_3Ce_6S_{14}$-type (hP24) and

0022-4596/97 $25.00

comprises an octahedrally coordinated first-row transition-metal or main-group metal M and a tetrahedrally coordinated main-group metal M'. These compounds have been predicted to undergo ferroelectric transitions at temperatures approaching 1000 K on the basis of the departure of M' from ideal tetrahedral coordination and the displacement of M from the center of its octahedron (23). However, the ferroelectric and nonlinear optical properties of these compounds have not yet been investigated. Here we report the synthesis and characterization of a new quaternary rare-earth sulfide that adopts the $Ln_6M_2M'_2S_{14}$ structure, $La_6(Mg_{0.5})_2Ge_2S_{14}$, as well as the synthesis and structure of a previously identified phase, $La_6(Mg_{0.5})_2Si_2S_{14}$ (21).

EXPERIMENTAL

Syntheses

Starting materials were used as received, except for La and CaS, which owing to their air sensitivity required initial purification. The lanthanum (Aldrich, 99.9%) was purified by drip melting under vacuum in an RF furnace, as described elsewhere (24). To remove any oxide, hydroxide, or other impurities, CaS (Johnson Matthey, 98%) was purified by flowing an Ar stream carrying S vapor over a boat of CaS in a flow tube heated to 800°C. All reactants were stored and handled in an Ar-filled glove box.

$La_6MgGe_2S_{14}$. Crystals of this composition were isolated from the reaction of stoichiometric amounts of La, Mg (Aldrich, 99.95%), Ge (Aldrich, 99.999%), and S in a $CaCl_2$/NaCl eutectic flux. This reaction was carried out in a vitreous carbon crucible sealed in an evacuated fused silica tube. The tube was heated slowly to 600°C over 48 h and held there for 12 h to allow for complete prereaction of the sulfur. This reduces the sulfur vapor pressure that otherwise could lead to explosions at higher temperatures. The temperature was then increased to 1000°C over 12 h and held there for 72 h. The tube was then slowly cooled (2°C/h) to 500°C at which point the furnace was shut off and allowed to cool to room temperature. The flux was washed away by soaking the product in distilled water for several hours. Transparent, orange-brown hexagonal needle-like crystals were obtained after filtration. The crystals were washed with more distilled water and dried in a dessicator. La_2S_3 was present as a minor phase. Electron microprobe measurements of these crystals on a JEOL 733 Superprobe indicated the presence of La, S, and Ge. Since the K-line of Mg overlaps with the L-line of Ge, a wavelength dispersive scan (WDX) that employed a crystal X-ray spectrometer was done to resolve the Mg and Ge peaks. This wavelength scan clearly showed both Mg and Ge peaks. Elemental analyses performed at Galbraith Laboratories, Knoxville, TN (25), using ICP also confirm the presence of Mg and Ge. For the Mg analysis, the material was dissolved in a combination of mineral acids (H_2SO_4, HNO_3, HF). Since Ge is lost as GeF_4 when dissolved in HF, lithium borate fusion techniques were used to dissolve the material for Ge analysis. The results, 1.65 wt% Mg and 9.8 wt% Ge, agree well with the values calculated for the $La_6MgGe_2S_{14}$ stoichiometry (Mg, 1.67 wt%, Ge 10.0 wt%). From single crystal X-ray diffraction structure determination, these crystals are $La_6MgGe_2S_{14}$.

$La_6MgSi_2S_{14}$. This material was obtained from the reaction of stoichiometric amounts of La, Mg, Si (Aldrich, 99.999%), and S in a NaCl/$MgCl_2$ flux in a vitreous carbon crucible sealed in an evacuated fused silica tube. The same heating profile and flux removal procedures described above were used. The major phase was $La_6MgSi_2S_{14}$ in the form of light-orange transparent crystals; however, minor secondary products, including La_2S_3, were also obtained. The electron microprobe analysis confirms the presence of La, Mg, Si, and S. From the single crystal X-ray data, these crystals are $La_6MgSi_2S_{14}$.

$La_6M_2Si_2S_{14}$ ($M = Na$, $0.5Ca$). Yellow needle-like crystals of what was thought to be "$La_6CaSi_2S_{14}$" were originally obtained after heating a nonstoichiometric mixture (1:1:1:4 molar ratio) of CaS, La, Si, and S in a NaCl/$CaCl_2$ eutectic flux in an alumina crucible sealed in fused silica. Subsequent electron microprobe measurements on a Hitachi SEM equipped with an EDX detector indicated the presence of aluminum in the crystals. Black needle-like crystals of what was thought to be "$La_6Na_2Si_2S_{14}$" were originally synthesized in a reaction that was intended to form $La_6BaSi_2S_{14}$. Elemental La, Si, and S were mixed with a eutectic NaCl/$BaCl_2$ flux in a graphite crucible, sealed in fused silica, and heated as previously described. It became clear in the structure refinement that barium was not present on the 2*a* site. Sodium was tried instead and it seemed to yield a reasonable refinement except that the Na–S bond lengths were very short (2.6 Å).

Additional attempts were made to prepare both "$La_6CaSi_2S_{14}$" and "$La_6Na_2Si_2S_{14}$" in Al-free environments. Stoichiometric amounts of La, CaS, (or Na_2S), Si, and S were combined with various eutectic halide salt fluxes in vitreous carbon crucibles and sealed in evacuated fused silica tubes. The tubes were heated as previously described (maximum temperature for attempted synthesis of Na phase, 900°C). Black to dark-red needles resulted in all cases. Electron microprobe experiments show only La, Si, and S. No Ca or Na is seen by this technique. A wavelength dispersive scan that used the crystal spectrometer on a JEOL733 Superprobe showed no conclusive evidence for the presence of Na in the nominally Na-containing crystal.

TABLE 1
Crystal Data and Intensity Collection for $La_6MgGe_2S_{14}$ and $La_6MgSi_2S_{14}$

Compound	$La_6MgGe_2S_{14}$	$La_6MgSi_2S_{14}$
Formula weight	1451.79	1362.79
space group	C_6^6-$P6_3$	C_6^6-$P6_3$
a (Å)[a]	10.367(1)	10.363(2)
c	5.814(1)	5.742(1)
Volume (Å^3), Z	541.09(8), 1	534.1(2), 1
Temperature (K)	293	293
Crystal size[b] (mm)	$\sim 0.028 \times \sim 0.028 \times \sim 0.028 \times \sim 0.11$	$0.053 \times 0.029 \times 0.029 \times 0.061$
Radiation	Mo$K\alpha$, graphite monochromated, $\lambda = 0.7093$ Å	Mo$K\alpha$, graphite monochromated, $\lambda = 0.7093$ Å
Linear abs. coeff., (cm^{-1})	157	132
Transmission factors	0.375–0.498[c]	0.518–0.613[d]
Scan type	θ–2θ	θ–2θ
θ Range	2.27–23.46°	2.27–27.49°
Reflections collected	3139	1989
Unique reflections, $R_{(int)}$	543, 0.0980	825, 0.0303
Goodness-of-fit on F^2	0.852	0.961
Variables, restraints	38, 1	38, 1
$R_w(F^2)$[e] (all data)	0.050	0.058
$R(F)$ ($F_o^2 > 2\sigma(F_o^2)$)	0.018	0.022
Absolute structure parameter	0.01(2)	−0.02(4)
Extinction coefficient	0.0182(9)	0.0174(8)
Largest diff. peak and hole, eÅ^{-3}	0.753, −0.719	2.695, −0.753

[a] The cell parameters were obtained from a refinement so that $a = b$, $\alpha = \beta = 90°$, $\gamma = 120°$.
[b] The first three dimensions given are the lengths of the edges of the approximately hexagonal cross section. The fourth value is the length of the crystal.
[c] Analytical absorption correction in the program XPREP was used (27).
[d] The empirical psi-scan absorption method in the program XPREP was used (27).
[e] $w^{-1} = \sigma^2(F_o^2) + (0.04 \times F_o^2)$ for $F_o^2 \geq 0$ and $w^{-1} = \sigma^2(F_o^2)$ for $F_o^2 < 0$.

Crystallographic studies

Precession photographs of $La_6MgSi_2S_{14}$ taken at 298 K display Laue symmetry 6/m and the systematic absence 00l, $l = 2n + 1$, consistent with the space groups C_6^6-$P6_3$ and C_{6h}^2-$P6_3/m$. Final lattice constants for the two compounds were determined from the least-squares analysis of the setting angles for 37 reflections centered at 298 K on a Siemens P4 diffractometer. Data were collected with the use of the Siemens XSCANS software (26). The intensities of three standard reflections monitored every 97 reflections during data collection were constant within counting statistics. An analytical absorption correction was utilized for $La_6MgGe_2S_{14}$ (see Table 1). An empirical ψ-scan absorption correction was applied to the 1989 observed reflections for $La_6MgSi_2S_{14}$ (825 unique reflections, $R_{(int)} = 0.0303$). Solutions were found in space group $P6_3$ with the direct methods program SHELXS in the SHELXTL PC system (27). Refinement made use of the program SHELXL-93 (27). In the final refinement of the structure, the values of the resultant R indices are as follows: $La_6MgGe_2S_{14}$ $-$ $R_w(F^2) = 0.050$, $R_1(F) = 0.018$ $(F_o^2 > 2\sigma(F_o^2))$; $La_6MgSi_2S_{14}$ $-$ $R_w(F^2) = 0.058$, $R_1(F) = 0.022$ $(F_o^2 > 2\sigma(F_o^2))$. The occupancy of the Mg atom in both $La_6MgGe_2S_{14}$ and $La_6MgSi_2S_{14}$ was fixed at $\frac{1}{2}$ to satisfy charge balance requirements. Allowing this value to vary had virtually no effect on the occupancy of the site (49.5% occupied) or the thermal parameters of that atom. The final structures were examined for additional symmetry with the MISSYM (28) algorithm in the PLATON (29) suite of programs. No symmetry other than that expected for the space group $P6_3$ was detected.

Values of the atomic parameters and equivalent isotropic displacement parameters for these structures appear in Tables 2 and 3. Selected bond lengths and angles appear in Tables 4. Final anisotropic displacement parameters and structure amplitudes are available as supplementary material.[1]

[1] See NAPS Document No. 05405 for 13 pages of supplementary materials. Order from ASIS/NAPS, Microfiche Publications, P.O. Box 3513, Grand Central Station, New York, NY 10163. Remit in advance $4.00 for microfiche copy or for photocopy, $7.75 up to 20 pages plus $0.30 for each additional page. All orders must be prepaid. Institutions and organizations may order by purchase order. However, there is a billing and handling charge of $15 for this service. Foreign orders add $4.50 for postage and handling for the first 20 pages, and $1.00 for each additional 10 pages of material. Add $1.50 for postage of any microfiche orders.

TABLE 2
Atomic Positions and Equivalent Isotropic Displacement Parameters for $La_6MgGe_2S_{14}$

Atom	Site	x	y	z	U(eq) (Å^2)[a]	Occ.
La	6*c*	0.3578(1)	0.1256(1)	0.7424(1)	0.010(1)	1
Mg	2*a*	0	0	0.4783(17)	0.009(1)	0.5
Ge	2*b*	2/3	1/3	0.3249(2)	0.008(1)	1
S(1)	6*c*	0.5211(1)	0.4133(1)	0.4741(3)	0.010(1)	1
S(2)	6*c*	0.0862(1)	0.8399(1)	0.7288(3)	0.012(1)	1
S(3)	2*b*	2/3	1/3	0.9519(5)	0.013(1)	1

[a] Here and in Table 3, U(eq) is defined as one-third of the trace of the orthogonalized U_{ij} tensor.

X-ray diffraction studies of the nominal crystals "$La_6CaSi_2S_{14}$" and "$La_6Na_2Si_2S_{14}$" show unit cell dimensions that are similar to those of $La_6MgSi_2S_{14}$, and refinements indicate the same atomic positions for La, Si, and S. Electron density, however, remains at the Mg site, as would be expected from charge balance arguments. Neither Ca nor Na is seen with EDX or WDX.

RESULTS AND DISCUSSION

The present compounds all exhibit the same structure type as the other members of the $Ln_6M_2M'_2S_{14}$ family (Figs 1 and 2). The structure contains one-dimensional chains of face-sharing MS_6 octahedra (M = Mg) running parallel to the 6_3 axis. These octahedra have crystallographically imposed three-fold symmetry. For both compounds, the M site is only half occupied. As there is no indication of a superstructure on the X-ray photographs we conclude that the distribution of M atoms in this site is random. The MgS_6 octahedra in $La_6MgGe_2S_{14}$ are regular with Mg–S distances of 2.672(6) and 2.675(5) Å. The octahedra in $La_6MgSi_2S_{14}$ are slightly more distorted with Mg–S bond lengths of 2.642(8) and 2.678(8) Å. All of the Mg–S distances are normal when compared to distances of 2.56–2.64 Å for Mg–S in MgS and Mg_2GeS_4 (30, 31).

These chains of octahedra are surrounded by isolated $M'S_4$ tetrahedra (M' = Si, Ge) that run along the three-fold axes. The GeS_4 tetrahedra in $La_6MgGe_2S_{14}$ are slightly distorted with Ge–S bond lengths of 2.168(3) and 2.229(1) Å. These values compare well with Ge–S bond distances of 2.134–2.222 Å found in Mg_2GeS_4 (31). The SiS_4 tetrahedra in $La_6MgSi_2S_{14}$ are also slightly distorted with Si–S bonds of 2.089(4) and 2.136(2) Å. These values are similar to the Si–S distance of 2.13 Å in the SiS_2 structure (32). In both

TABLE 3
Atomic Positions and Equivalent Isotropic Displacement Parameters for $La_6MgSi_2S_{14}$

Atom	Site	x	y	z	U(eq) (Å^2)[a]	Occ.
La	6*c*	0.1221(1)	0.3577(1)	0.2933(1)	0.008(1)	1
Mg	2*a*	0	0	0.0381(25)	0.012(1)	0.5
Si	2*b*	1/3	2/3	0.8775(5)	0.008(1)	1
S(1)	6*c*	0.4086(2)	0.5248(2)	0.0172(2)	0.009(1)	1
S(2)	6*c*	0.8371(2)	0.0822(2)	0.2822(4)	0.010(1)	1
S(3)	2*b*	1/3	2/3	0.5137(5)	0.010(1)	1

TABLE 4
Selected Bond Lengths (Å) and Angles (deg.) for $La_6MgGe_2S_{14}$ and $La_6MgSi_2S_{14}$

$La_6MgGe_2S_{14}$		$La_6MgSi_2S_{14}$	
La-S(2)	2.887(1)	La–S(2)	2.877(1)
La–S(2)	2.893(1)	La–-S(2)	2.907(1)
La–S(1)	2.922(1)	La–S(1)	2.921(2)
La–S(2)	3.004(2)	La–S(2)	2.989(2)
La–S(1)	3.024(1)	La–S(1)	3.031(2)
La–S(1)	3.065(1)	La–S(1)	3.055(2)
La–S(3)	3.079(1)	La–S(3)	3.104(1)
La–S(2)	3.154(2)	La–S(2)	3.108(2)
Mg–S(2)	2.672(6) × 3	Mg–S(2)	2.642(8) × 3
Mg–S(2)	2.675(5) × 3	Mg–S(2)	2.678(8) × 3
Ge–S(3)	2.168(3)	Si–S(3)	2.089(4)
Ge-S(1)	2.229(1) × 3	Si–S(1)	2.136(2) × 3
S(1)–Ge–S(3)	112.89(5) × 3	S(1)–Si–S(3)	112.06(9) × 3
S(1)–Ge–S(1)	105.84(6) × 3	S(1)–Si–S(1)	106.76(9) × 3

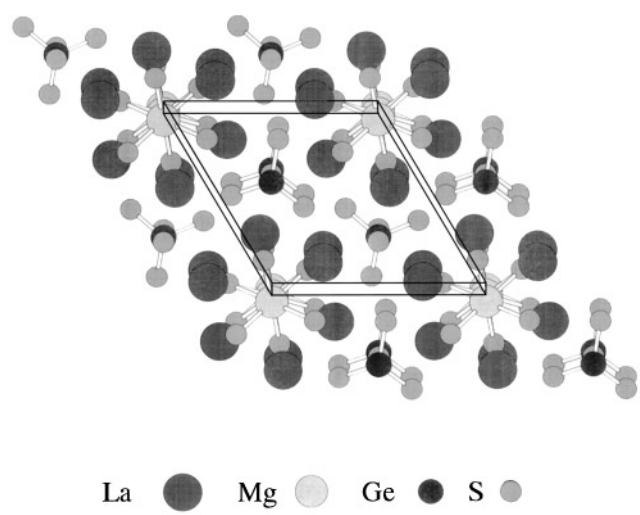

FIG. 1. Structure of $La_6MgGe_2S_{14}$ as viewed down [001] (35). The structure of $La_6MgSi_2S_{14}$ is analogous except that the crystal selected has its polar axis reversed.

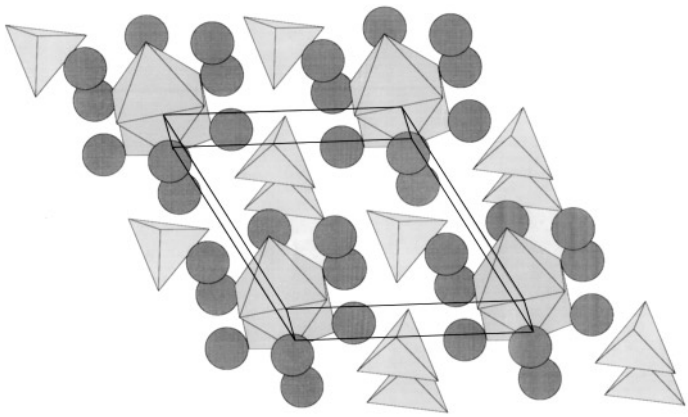

FIG. 2. Polyhedral representation of $La_6MgGe_2S_{14}$ (35) tipped slightly from [001] to show the isolated GeS_4 tetrahedra and the chains of MgS_6 octahedra. Lanthanum atoms are represented by circles.

cases, the shorter bond is along the three-fold axis. The structure is polar with all of the GeS_4 tetrahedra pointing in the same direction.

The La atom is in a square-antiprismatic environment, filling space between the Mg and Si or Ge polyhedra. The La–S bond lengths in $La_6MgGe_2S_{14}$ range from 2.887(1)–3.154(2) Å and those in $La_6MgSi_2S_{14}$ range from 2.877(1)–3.108(2) Å. These may be compared with La–S distances in LaS_2 of 2.903(2)–3.232(3) Å (33).

There is neither metal–metal bonding nor sulfur–sulfur bonding in these structures, the shortest S–S distance being longer than 3.4 Å. Consequently, in these compounds formal oxidation states of La^{3+}, Mg^{2+}, Si^{4+}, Ge^{4+}, and S^{2-} may be assigned.

We cannot conclusively determine the composition or structure of "$La_6M_2Si_2S_{14}$" ($M = Na, 0.5Ca$). Electron microprobe analysis indicates the presence of only La, Si, and S in the crystals synthesized in vitreous carbon crucibles. Both crystals have the same La, Si, S framework structure as $La_6MgGe_2S_{14}$, and clearly have electron density on the 2*a* site. Several models were tried to account for this residual electron density. In the first, we assumed the site contains 0.5 Si^{2+} (an oxidation state observed in related germanium compounds (34)), since this charge/occupancy leads to charge balance. While the refinement *R* indices are good ($R_1 = 0.026$, $R_w = 0.088$), the thermal parameters for Si on the 2*a* site are very small, indicating that not enough charge density is on the site. If the Si occupancy at 2*a* is unconstrained, the site occupancy increases to 0.78 and $R_1 = 0.016$ and $R_w = 0.051$. These differences in the *R* indices between these models are probably significant. However, this second model does not lead to sensible oxidation states. The deep red/black color of the crystals suggests a different electronic structure from that of $La_6MgSi_2S_{14}$, as might be expected if defects are present. Such defects could lead to a sensible charge balance. Electron microprobe measurements were not quantitative enough to verify the presence of Si on the 2*a* site.

Preliminary NLO studies are not encouraging. When a powdered sample of $La_6MgSi_2S_{14}$ was irradiated with light from a commercial Nd–YAG laser operating at 10 Hz with a fundamental at 1.064 μm, no second harmonic generation was visible. In this experiment, green light should have been produced at 532 nm, as is typical for most materials with reasonable NLO susceptibilities, especially if appropriate phase-matching conditions are met. To investigate fully the potential nonlinear optical properties of these materials, more careful studies that address issues such as input intensity, phase-matching, and conversion efficiency would have to be undertaken on much larger crystals. With bigger crystals and better yields, the ferroelectric properties of these materials could also be investigated.

ACKNOWLEDGMENTS

The research at Cornell University was supported by DOE Grant DE-FG02-87ER45298 and at Northwestern University by NSF Grant DMR 91-14934. RLG and CMS thank John Hunt of the Cornell M.S.C. Electron Microscopy Labs for his assistance with the microprobe measurements, Emil Lobkovsky of the Cornell Department of Chemistry Crystallography Facility for his assistance with some of the single crystal X-ray work, Simon J. Clarke for his help with some of the single crystal work, Randall J. Lane for his assistance with the non-linear optical studies, and Donna Smith for her EDX work at Northwestern University.

REFERENCES

1. S. R. Marder, J. E. Sohn, and G. D. Stucky (Eds.), "Materials for Nonlinear Optics," ACS Symposium Series, Vol. 455, American Chemical Society, Washington, D.C., 1991.
2. K. J. Sunders, T. Y. Wong, T. M. Hartnett, R. W. Tustison, and R. L. Gentilman, *Proc. SPIE-Int. Soc. Opt. Eng.* **683,** 72 (1986).
3. P. N. Kumta and S. H. Risbud, *J. Mater. Res.* **8,** 1394 (1993).
4. I. V. Fekeshagazi, K. V. May, V. M. Mitsa, and Yu. V. Vlasenko, *Proc. SPIE-Int. Soc. Opt. Eng.* **1983,** 834 (1993).
5. C. E. Miller, W. C. Eckhoff, U. Simon, F. K. Tittel, and R. F. Curl, *Proc. SPIE-Int. Soc. Opt. Eng.* **2145,** 282 (1994).
6. C. K. Bucher and S.-J. Hwu, *Inorg. Chem.* **33,** 5831 (1994).
7. R. L. Gitzendanner and F. J. DiSalvo, *Inorg. Chem.* **35,** 2623 (1996).
8. J. D. Carpenter and S.-J. Hwu, *Chem. Mater.* **4,** 1368 (1992).
9. A. E. Christuk, P. Wu, and J. A. Ibers, *J. Solid State. Chem.* **110,** 330 (1994).
10. P. J. Walker and R. C. C. Ward, *Mat. Res. Bull.* **19,** 717 (1984).
11. B.-H. Chen, B. W. Eichhorn, and P. E. Fanwick, *Inorg. Chem.* **31,** 1788 (1992).
12. H. J. Scheel, *J. Cryst. Growth* **24,** 669 (1974).
13. W. Bronger and O. Günther, *J. Less-Common Met.* **27,** 73 (1972).
14. M. Guittard, M. Julien-Pouzol, P. Laruelle, and J. Flahaut, *C. R. Acad. Sci. Paris Sér. C* **267,** 767 (1968).
15. A. Michelet and J. Flahaut, *C. R. Acad. Sci. Paris Sér. C* **269,** 1203 (1969).
16. G. Collin and P. Laruelle, *C. R. Acad. Sci. Paris Sér. C* **270,** 410 (1970).
17. G. Collin and J. Flahaut, *C. R. Acad. Sci. Paris Sér. C* **270,** 488 (1970).

18. G. Perez, M. Darriet-Duale and P. Hagenmuller, *J. Solid State Chem.* **2,** 42 (1970).
19. N. Rodier, M. Guittard, and J. Flahaut, *C.R. Acad. Sci. Paris Sér. C* **296,** 65 (1983).
20. K. S. Nanjundaswamy and J. Gopalakrishnan, *J. Solid State Chem.* **49,** 51 (1983).
21. J. Flahaut and P. Laruelle, *in* "The Chemistry of Extended Defects in Non-metallic Solids," (L. Eyring and M. O'Keeffe, Eds.), p. 109, North-Holland, Amsterdam, 1970.
22. S. Jaulmes, M. Palazzi, and P. Laruelle, *Mater. Res. Bull.* **23,** 831 (1988).
23. S. C. Abrahams, *Acta Crystallogr. Sect. B* **46,** 311 (1990).
24. R. A. Gordon, Y. Ijiri, C. M. Spencer, and F. J. DiSalvo, *J. Alloys Compd.* **224,** 101 (1995).
25. Galbraith Laboratories, 2323 Sycamore Drive, Knoxville, TN 37921-1750.
26. "XSCANS Single Crystal Data Collection Software," Version 2.10B, Siemens Analytical X-ray Instruments, Inc.
27. G. M. Sheldrick, "SHELXTL," PC Version 5.0 [An integrated system for solving, refining, and displaying crystal structures from diffraction data]. Siemens Analytical X-Ray Instruments, Inc. Madison, WI, 1994; Sheldrick, G. M., *Acta Crystallogr., Sect. A: Found. Crystallogr.*, **46,** 467, (1990).
28. Y. Le Page, *J. Appl. Crystallogr.* **20,** 264 (1987).
29. A. L. Spek, *Acta Crystallogr., Sect. A: Found. Crystallogr.* **46,** C34 (1990).
30. O. J. Guntert and A. Faessler, *Z. Krist.* **107,** 357 (1956).
31. H. Vincent and G. Perrault, *Bull. Soc. Fr. Mineral. Cristallogr.* **94,** 551 (1971).
32. C. T. Prewitt and H. S. Young, *Science* **149,** 535 (1965).
33. J. Dugué, D. Carré, and M. Guittard, *Acta Crystallogr. Sect. B* **34,** 403 (1978).
34. A. Michelet and J. Flahaut, *C. R. Acad. Sci. Paris Sér. C* **268,** 326 (1969).
35. Figures were drawn with the program ATOMS v3.1β, Shape Software.